Atmospheric Environment 44 (2010) 2316–2329

Contents lists available at ScienceDirect

Atmospheric Environment

journal homepage: www.elsevier.com/locate/atmosenv

Evaluation of aerosol sources at European high altitude background sites with trajectory statistical methods

Pedro Salvador [a,*], Begoña Artíñano [a], Casimiro Pio [b], Joana Afonso [b], Michel Legrand [c], Hans Puxbaum [d], Samuel Hammer [e]

[a] Department of Environment, Edf. 23. CIEMAT. Avda. Complutense 22, 28040 Madrid, Spain
[b] CESAM & Department of Environment, University of Aveiro, Portugal
[c] Laboratoire de Glaciologie et Geophysique de l'Environment, CNRS, France
[d] Institute for Chemical Technologies and Analytics, Technical University of Vienna, Austria
[e] Institut fur Umweltsik, University of Heidelberg, Germany

ARTICLE INFO

Article history:
Received 6 October 2009
Received in revised form
30 March 2010
Accepted 31 March 2010

Keywords:
Trajectory statistical methods
Cluster analysis
Redistributed concentration field method
Geochemistry
Long-range transport
PM10
PM2.5

ABSTRACT

This study has investigated the influence of synoptic weather patterns and long-range transport episodes on the concentrations of several compounds related to different aerosol sources (EC, OC, SO_4^{2-}, Ca^{2+}, Na^+, K^+, ^{210}Pb, levoglucosan and dicarboxylic acids) registered in PM10 or PM2.5 aerosol samples collected at three remote background sites in central Europe. Air mass back-trajectories arriving at these sites have been analysed by statistical methods. Firstly, air mass back-trajectories have been grouped into clusters. Each cluster corresponds to specific meteorological scenarios, which were extracted and discussed. Finally, redistributed concentration fields have been computed to identify the main potential source regions of the different key aerosol components. A marked seasonal pattern is observed in the occurrence of the different clusters, with fast westerly and northerly Atlantic flows during winter and weak circulation flows in summer. Spring and fall were characterised by advection of moderate flows from northeastern and eastern Europe. Significant inter-cluster differences were observed for concentrations of receptor aerosol components, with the highest concentrations of EC, OC, SO_4^{2-}, K^+ and ^{210}Pb associated with local and mesoscale aerosol sources located over central Europe related to enhanced photochemical processes. Emissions produced by fossil fuel and biomass burning processes from the Baltic countries, Byelorussia, western regions of Russia and Kazakhstan in spring and fall also contribute to elevated levels of EC, OC, SO_4^{2-}, K^+ and ^{210}Pb. In the summer period long-range transport episodes of mineral dust from North-African deserts were also frequently detected, which caused elevated concentrations of coarse Ca^{2+} at sites. The baseline aerosol concentrations in central Europe at the high altitude background sites were registered in winter, with the exception of coarse Na^+. While the relatively high concentrations of Na^+ can be explained by sea salt advected from the Atlantic, the low levels of other aerosol components are caused by efficient aerosol scavenging associated to advections of Atlantic air masses, as well as lower emissions of these species over the Atlantic compared to those over the European continent and very limited vertical air mass exchange over the continent.

1. Introduction

The temporal variability of atmospheric particulate matter (PM) concentrations at a monitoring site is highly related to the history of the air mass arriving at that site. Therefore numerous studies of atmospheric PM levels have applied trajectory statistical methods (TSM), which allow simultaneous computational treatment of air mass back-trajectories and of PM concentrations at one or several receptor points.

The analysis of a large number of back-trajectories of air masses arriving at receptor sites is a valuable tool for investigating the sources and origins of particulate matter at those sites. Subsequently, cluster analysis can be used to group trajectories into homogeneous groups, depending on direction and speed of transport (Dorling et al., 1992; Brankov et al., 1998; Salvador et al., 2008). Furthermore, the synoptic meteorological scenarios associated to each cluster can be extracted from the analysis and used to highlight the fluctuations of the aerosol load and composition at sites.

* Corresponding author. Tel.: +34 91 3466174; fax: +34 91 3466212.
E-mail address: pedro.salvador@ciemat.es (P. Salvador).

1352-2310/$ – see front matter © 2010 Elsevier Ltd. All rights reserved.
doi:10.1016/j.atmosenv.2010.03.042

TSM also permit to identify geographical areas associated with very low and high concentrations of PM components. Thus, they can be interpreted as potential sink and source regions, or also as preferred air mass transport pathways (Stohl, 1998). Although they do not consider effects such as atmospheric dispersion, chemical conversion, or dry and wet deposition, TSM are easy to apply and powerful, identifying the relevant source regions and the air flow regimes which are associated with regional and large-scale air pollution transport. As discussed by Viana et al. (2008), receptor modelling techniques using back-trajectory analysis (alone and in combination with other receptor modelling) have been applied only by a relatively low number of research teams in Europe (Viana et al., 2008 and references therein). Because TSM holds great potential for identifying potential source regions of PM, these authors encouraged their use in PM source apportionment studies. The use of TSM deploying large trajectory ensembles can significantly reduce the trajectory uncertainty (random errors) generated by interpolation and truncation processes, low temporal or spatial resolution of wind data, or an inappropriate selection of the starting heights, and permits important improvements in the predictability of TSM (Stohl, 1998; Lupu and Maenhaut, 2002).

Cluster Analysis (CA) can be used to classify the air mass origins that arrive at a site, but CA does not provide any information on the geographical location of potential source regions. This information can be obtained by applying the Redistributed Concentration Field method (RCF) (Stohl, 1996). This technique has already been applied to locate potential source regions for PM components (Stohl, 1996; Salvador et al., 2007), acidic species in precipitation (Charron et al., 1998) or heavy metals (Han et al., 2004). Wotawa and Kröger (1999) successfully tested the ability of the RCF method to reproduce emission inventories of air pollutants.

On the basis of a 2-year aerosol data set obtained within the CARBOSOL European project (Present and Retrospective State of Organic Aerosol over Europe), many important issues related to sources of PM10 and PM2.5 (particles with aerodynamic size lower than 10 and 2.5 μm, respectively) have been discussed and evaluated (Legrand and Puxbaum, 2007). An important outcome of CARBOSOL was to provide a comprehensive data set on inorganic and carbonaceous aerosol constituents at rural and background sites in Europe (Pio et al., 2007). These data were discussed versus environmental conditions at sites (marine versus continental, rural versus forested, boundary layer versus free troposphere, and winter versus summer) for elemental and organic carbon (EC and OC), major inorganic ions (Pio et al., 2007) and some specific organic species such as C2-C5 dicarboxylic acids (Legrand et al., 2007) or levoglucosan (Puxbaum et al., 2007). A seasonal source apportionment of PM2.5 organic aerosol was also performed (Gelencsér et al., 2007). Current EMEP models have been used to simulate sulfate and OC (Simpson et al., 2007) and EC (Tsyro et al., 2007) concentrations over Europe and data were compared with observations made during CARBOSOL.

Up to now CARBOSOL data have not been examined in terms of source regions and transport pathways for the different aerosol fractions. Only Fagerli et al. (2007) performed source–receptor calculations with the EMEP model to allocate sulfate and ammonium sources at the top of the Alps with the aim to discuss their ice core records. TSM would nicely complement the dispersion modelling approach previously applied to the CARBOSOL data set.

In this work we have first applied a cluster analysis to classify the air mass origins that arrive at three continental background sites where the climatology of aerosol was established during CARBOSOL. Then, the meteorological scenarios associated to each cluster were extracted and their impact on particle concentrations and composition at sites evaluated. Finally, the redistributed concentration field method was also applied.

2. Methodology

2.1. CARBOSOL sampling sites and data

In the framework of the CARBOSOL European project, atmospheric aerosol was continuously sampled for 2 years at 6 monitoring sites in Europe (Pio et al., 2007). Three of these sites are located in the centre of Europe (Fig. 1) and can be classified as natural continental background: Schauinsland-SIL in Germany (47°55′N, 07°54′E, 1205 m asl), Puy de Dôme-PDD in France (45°46′N, 02°57′E, 1450 m asl) and Sonnblick-SBO in Austria (47°03′N, 12°57′E, 3106 m asl). PDD and SIL are medium-elevation mountain stations; PDD is situated at an isolated mountain top in central France, whereas SIL is located on a mountain ridge of the Black Forest in southwestern Germany. The high altitude SBO observatory is situated on an isolated peak of the glaciered East Alpine ridge and most of the time is located within the free troposphere (Kasper and Puxbaum, 1998). Since TSM are powerful at receptor sites not strongly impacted by local or mesoscale impurity sources, we restrict our study to these 3 sites where no significant local sources exist, unlike the other 3 low altitude CARBOSOL sites where local sources do exist (Pio et al., 2007).

Monitoring of gases and aerosol composition (Kasper and Puxbaum, 1998; Seibert et al., 1998; Tscherwenka et al., 1998; Kaiser et al., 2007) and more recently aerosol size distributions (Venzac et al., 2009) has been previously performed at European

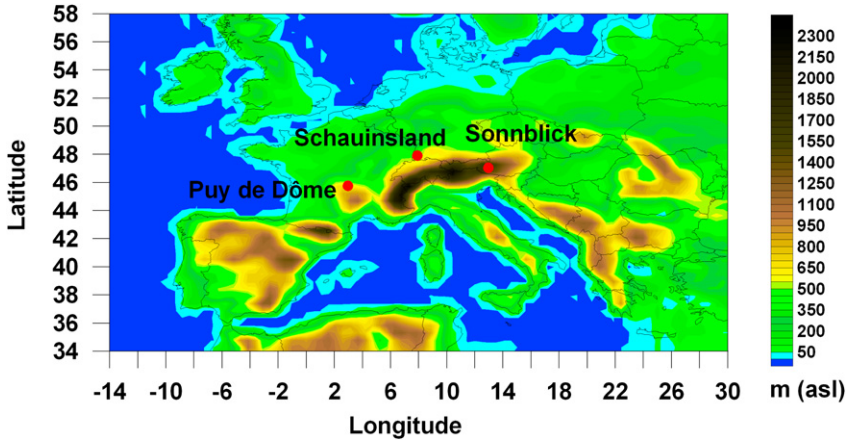

Fig. 1. Map of Europe detailing the position of the three CARBOSOL high altitude background sampling sites.

mountain sites. The present paper uses a more comprehensive data set of specific tracers of aerosol sources, such as ^{210}Pb or levoglucosan, which were not routinely determined in these previous air quality monitoring studies. At SIL, PDD and SBO, the aerosol sampling was performed from October 2002 to October 2004. Aerosol samples were collected on quartz fibre filters with high volume sampler equipped with PM10 (SIL and PDD) or PM2.5 (SBO) inlets. The sampling periods frequently lasted for one week. Filter samples were analyzed for aerosol carbonaceous fractions (EC, OC, water-soluble inorganic ions including SO_4^{2-}, NO_3^-, NH_4^+, Ca^{2+}, K^+, Mg^{2+}, Cl^-, and Na^+). Additionally, analyses of specific organic compounds (C2–C5 dicarboxylic acids, levoglucosan, etc.) and ^{210}Pb were also carried out. The detailed description of the sampling sites, sampling and analysis can be found elsewhere (Pio et al., 2007). The number of collected and analysed PM filters is 87, 96, and 104 at PDD, SBO, and SIL, respectively. In this paper the warm season refers to the months from April to September and the cold season to the six remaining months of the year.

In this work we focused on the impact of air flow regimes on the levels of the most important inorganic and organic aerosol components, namely EC, OC, SO_4^{2-}, Ca^{2+}, Na^+, K^+ and ^{210}Pb. EC and OC are the two main fractions in which atmospheric particulate carbon is usually classified. EC is essentially primarily emitted, during the incomplete combustion of fossil and biomass carbonaceous fuels. Anthropogenic primary OC is also formed during fossil fuel combustion. Primary biogenic OC aerosol sources consist of plant debris, humic matter, pollens and microbial particles, and products of incomplete combustion of biomass. Secondary organic aerosol (SOA) is formed from gas-to-particle conversion of semi-volatile organic compounds (biogenic and anthropogenic) in the atmosphere. SO_4^{2-} is the most relevant secondary inorganic aerosol in the atmosphere. Na^+ and Ca^{2+} are representative of the sea salt and crustal primary aerosols, respectively. Ca^{2+} concentrations obtained at SBO were not used in this study because the samples were probably contaminated by concrete (Pio et al., 2007).

^{210}Pb is secondarily produced from a precursor gas, ^{222}Rn, which is emitted at a relatively uniform and constant rate from the soil (Hammer et al., 2007). The ^{210}Pb is attached to aerosol particles in the submicron size range in the atmosphere and mineral dust aerosol can make at most 10% of the ^{210}Pb load derived from airborne ^{222}Rn (Hammer et al., 2007). Its variability is mainly governed by atmospheric transport processes, which is why it is regarded as a good tracer of the transport and permanence of air masses over continental regions.

K^+ can be related to sea salt and mineral dust, as well as to wood burning emissions. However, it was shown that at the continental CARBOSOL sites a dominant fraction of K^+ was present in the submicron size fractions and thus could not be attributed to sea salt or mineral dust (Pio et al., 2007). A large fraction of K^+ is thus thought to be related to wood burning.

Additional analyses include levoglucosan as a proxy of biomass smoke (Puxbaum et al., 2007) and C2–C5 dicarboxylic acids thought to be possibly representative of secondary organic aerosol (Legrand et al., 2007). Levoglucosan measurements were made by weekly sampling in winter and with monthly pooled filters during summer. Consequently, only winter samples were used in our analyses.

2.2. Trajectory statistical methods

5-day backward air trajectories arriving at SIL, PDD and SBO sites were used and analysed together with the concentrations of PM components recorded there. For each day, four 3-D trajectories ending at 00:00, 06:00, 12:00 and 18:00 UTC were computed by the Norwegian Institute for Air Research NILU (SIL and PDD) and the Central Institute for Meteorology and Geophysics of Austria (SBO) using the FLEXTRA model (Stohl et al., 1995) and meteorological data provided from ECMWF (European Centre for Medium-Range Weather Forecasts). Fixed heights of 1465 m, 1700 m and 3105 m asl were chosen as the air masses arrival heights for PDD, SIL and SBO respectively. These altitudes were selected because they approximately coincide with the standard meteorological charts of geopotential height at 850 hPa (1500 m asl) and 700 hPa (3000 m asl). They are representative heights of the mean transport wind at a synoptic scale (Stohl, 1998). In total, more than 8000 complete trajectories were used for analysis, each with 40 endpoints. For any sample, the endpoints of all the trajectories calculated for each day of the sampling period, were combined into a single composed trajectory. Because of the weekly sampling, those samples which were influenced by many different air mass origins were not included in our analysis. With this aim a centroid was computed representing the averaged flow of the complete back-trajectory group for each day of the sampling period. In order to assess quantitatively the deviation of any back-trajectory of the group from the corresponding centroid, the relative horizontal transport deviation RHTD (Stohl et al., 1995) between them was computed. When the RHTD for any individual trajectory exceeded the 50% it was concluded that it has a substantial different origin than the averaged flow represented by the centroid (Jorba et al., 2004). Therefore composed trajectories, in which more than 40% of individual trajectories were found to have substantially different origins, were discarded from the trajectory analysis. As a result, 32 aerosol samples were excluded from the dataset, leaving a total of 255 events.

Firstly, air mass back-trajectories were grouped into clusters, each one representing a characteristic meteorological scenario. Trajectory endpoints were used as the clustering variables. A non-hierarchical method known as the k-means procedure was applied. As detailed in Owen (2003) this iterative algorithm uses a specified number of clusters, k, to partition the data by comparing each object to the arithmetic mean of all the members of each of the k clusters (cluster centres). The selection of the optimal number of clusters that best describes the different air flow patterns was performed by computing the percentage change in within-cluster variance, as a function of the number of clusters (Dorling et al., 1992; Brankov et al., 1998; Salvador et al., 2008). The optimum number of clusters retained was 7, 8 and 8 for SBO, PDD and SIL, respectively.

Once the CA were performed, composite synoptic maps were calculated by averaging the sea level pressure and the geopotential height at the 850 hPa topography, using the data corresponding to all days in which back-trajectories were assigned to a particular cluster. The meteorological variables used were obtained from the NCEP/NCAR Reanalysis datasets files (Kalnay et al., 1996), provided by the NOAA/OAR/ESRL PSD, USA. Next, mean EC, OC, SO_4^{2-}, Ca^{2+}, Na^+, ^{210}Pb and K^+ concentrations were calculated for all trajectory clusters arriving at PDD, SIL and SBO. The non-parametric Kruskal–Wallis test was used to test the significance of inter-cluster variation in PM concentration. This technique tests the null hypothesis that several samples have been drawn from the same population. If the test leads to the rejection of the null hypothesis, it is interpreted as follows: PM levels are influenced by the transport paths of air masses arriving at this site, which are represented by the clusters. To find out which clusters are significantly different from which others, the Dunn test for multiple sample comparison was used in this work (Brankov et al., 1998; Salvador et al., 2008).

Finally, RCFs, as defined by Stohl (1996), have been computed. A 2° longitude × 2° latitude cells grid has been superimposed over the region defined by 18°N – 72°N and 27°W – 57°E. For each ij-th grid cell a weighted concentration C_{ij} was computed.

This technique combines air back-trajectory information and concentrations of the components measured at the sampling places as detailed in Stohl (1996). RCFs have thus been computed for SBO (PM2.5) and for SIL and PDD together (PM10), for the whole sampling period and also for the warm and cold seasons. Lupu and Maenhaut (2002) have advocated the calculation of the RCF with data from different locations, with the aim of improving their spatial resolution. It must be pointed out that only those source regions that have effects on the measured air pollutant data can be detected with these methods. The RCF methodology used in this paper can detect only those source areas of the pollutant investigated that are able to potentially influence its concentration levels registered at the monitoring site by regional or long-range transport episodes. Vinogradova (2000) showed that the most polluting source contributing to an observation point by medium- or long-range transport, may not be the one with the highest emission level. This depends on the specific air mass transport patterns which affect each site and the residence time of the air masses over the potential source areas.

3. Results and discussion

3.1. Cluster analysis results

3.1.1. Characterisation and seasonal evolution of the clusters

As seen in Fig. 2 the final cluster centers after the last iteration in the clustering procedure at SBO, PDD and SIL were quite similar, despite some minor cluster differences from one site to another. Zonal flows accounted for most of data at the 3 sites (46% at PDD, 50% at SIL and SBO). They correspond to fast westerly flows from the mid Atlantic Ocean (cluster 1), moderately fast southwesterly (cluster 2) and fast north-westerly flows (clusters 3). The fastest flows (cluster 1) more frequently took place at the highest altitude site of SBO.

The slowest flows accounted for from 29 to 33% of cases. Cluster 4 represented a slow moving north-westerly flow for SBO (20%) and SIL (16%), whereas it gathered southwesterly trajectories slowly moving from the Iberian Peninsula and the south of France for PDD (18%). Due to its geographical position, PDD was under a higher influence of southern flows than SIL and SBO; the Alpine range protecting these sites, especially at higher altitudes, from the direct influence of southern flows during low baric gradient situations. Slow north-easterly flows (cluster 5) accounted for 14%, 17% and 9% of the trajectories at PDD, SIL and SBO, respectively. A clear displacement of the flows represented by the cluster 5 towards the east, was featured from PDD, to SIL and SBO.

Cluster 6 indicated a moderate rapid flow moving to central Europe from Russia, the Baltic countries and Ukraine. The eastern European flows represented by this cluster, accounted for 4% of the trajectories at SBO and 5% at PDD and SIL. Moderate fast moving trajectories coming from the western and central Mediterranean basin and the North of Africa were grouped in cluster 7. This cluster represented 9%, 12% and 17% of the data at SIL, PDD and SBO, respectively. Northerly flows moving fast along the North European coastal corridor were grouped in cluster 8 for PDD and SIL only. This transport regime is not frequent (5% at PDD, 2% at SIL), and is not detected at SBO.

In winter the most frequent regimes were Atlantic advection flows (clusters 1 and 2) (Fig. 3a-b). The most common meteorological scenarios causing these flows were characterised by strong longitudinal baric gradients, observed when the Azores high was shifted to the southeast of its normal position and a deep low was centred northeast of the Canadian coast (Fig. 4a-b). Fast north-westerly flows (clusters 3) occurred more frequently during winter and autumn and only sporadically during spring and summer (Fig. 3c). The meteorological scenario causing these flows in winter was associated with a shift of the Azores high towards the north and the presence of a trough over the Mediterranean Sea (Fig. 4c).

Moderate and slow moving trajectories represented by cluster 4 occurred predominantly in summer (Fig. 3d). During this season the European continent was frequently under low baric gradient situations, as seen in Fig. 4d. These meteorological scenarios were characterised by a lack of significant air mass advection, the prevalence of regional atmospheric circulations (sea breezes, up-slope and down-slope winds, or valley winds) and the enhancement of the mixed layer development under high insolation conditions. Kasper and Puxbaum (1998) showed how during bright summer afternoons, when the mixing height is well above the SBO site, vertical mixing leaded to an exchange between boundary layer air and free tropospheric air masses and the formation of a modified mixing layer. Venzac et al. (2009) confirmed that the air reaching the PDD sampling site is strongly influenced by the boundary layer during the day in summer.

The transition period between the occurrence of the longest trajectories in winter and the shortest ones in summer was characterised by the advection of slow and moderate flows from northeastern (cluster 5) and eastern (cluster 6) European regions (Fig. 3e-f). These flows were induced by the presence of a strong high pressure system between the British Islands and the Baltic countries (Fig. 4e–f). In the case of the flows represented by cluster 6, the high pressure system was shifted towards the south and a deep low was placed over the eastern border of the Mediterranean sea (Fig. 4f). This meteorological scenario greatly favoured the advection of air masses from the east to the centre of the continent.

Meteorological scenarios favouring the transport of air masses from the Mediterranean basin and the northern regions of Africa to the centre of Europe (cluster 7), also occurred in the summer and the early autumn months (Fig. 3g) The intense heating of the North-African surface during these months frequently generated the development of a thermal low, which pumped dust into the mid-troposphere. A compensatory high pressure system was formed in the upper atmospheric levels (850 hPa), the dust being transported towards the continent through its western branch (Fig. 4g).

The rare trajectories grouped in cluster 8 occurred predominantly in winter (Fig. 3h). This cluster was characterised by fast northerly flows over the centre of Europe and were produced by the combination of the Azores high, shifted to the north, while a deep low stayed over the north of Norway (Fig. 4h).

3.1.2. Influence of the clusters on PM levels

The mean concentrations of EC, OC, SO_4^{2-}, Ca^{2+}, K^+, Na^+ and ^{210}Pb for all trajectory clusters arriving at PDD, SIL and SBO, are summarized in Table 1. Kruskal–Wallis non-parametric tests indicated that statistically significant differences in all receptor PM components concentrations, were observed for the different air mass transport patterns at the 95% confidence level. The Dunn test for multiple sample comparison was used to find out which clusters were significantly different from which others.

The mean EC, OC, SO_4^{2-}, ^{210}Pb and K^+ concentrations associated with slow and moderate moving flows (clusters 4 and 5) were significantly higher than mean concentrations observed for the other trajectory categories at all sites. These synoptic meteorological situations were characterised by the prevalence of recirculation of air mass under weak baric gradient situations. The persistence of these scenarios favoured transport from local and regional continental sources (Kasper and Puxbaum, 1998; Seibert et al., 1998), fumigation of emission plumes from industrial areas, formation of secondary compounds by photochemical conversion and turbulence and convective dynamics that cause the re-suspension of soil particles (Salvador et al., 2007; Querol et al., 2008a).

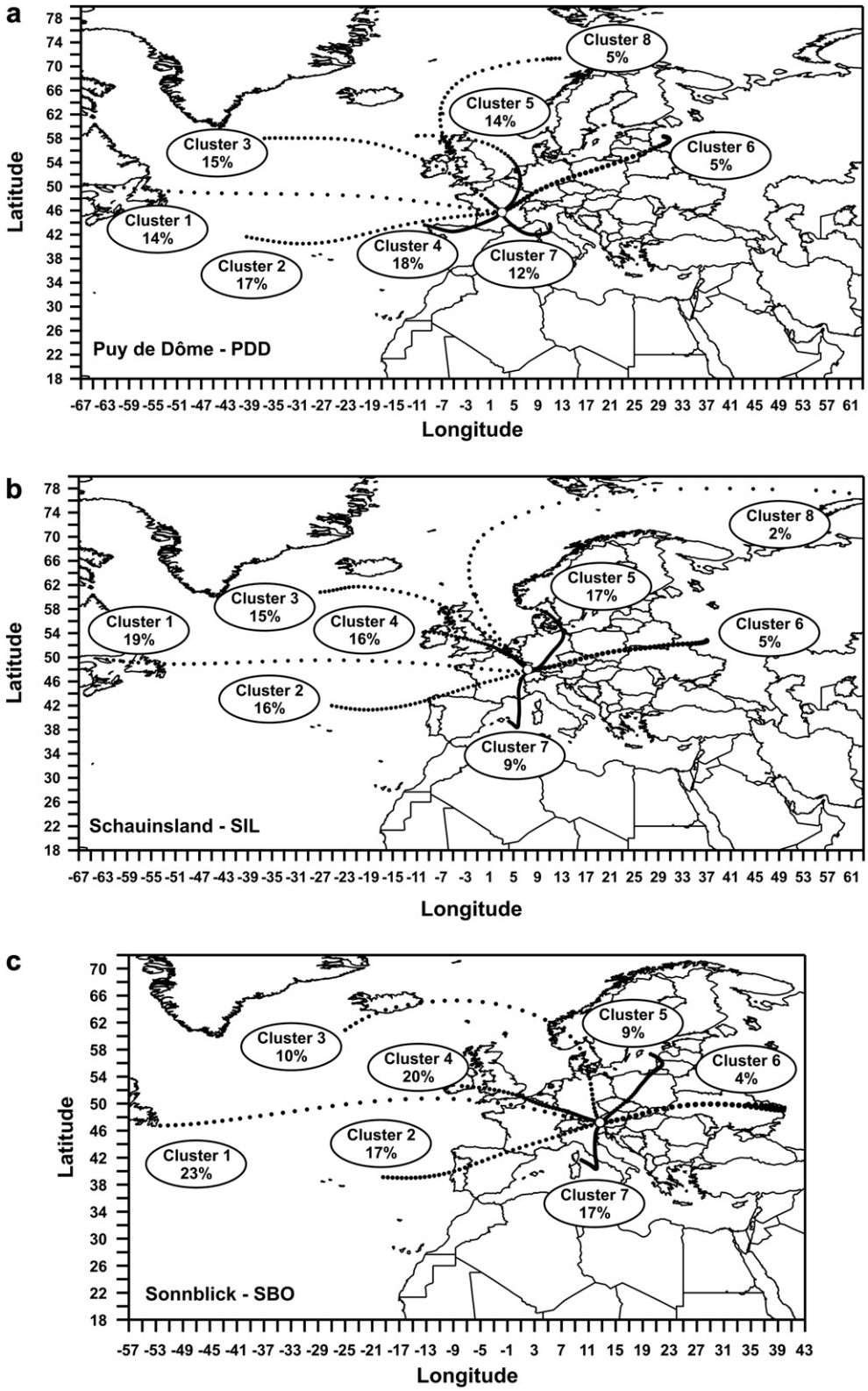

Fig. 2. Cluster centres resulting from the analysis are shown. The percentage of trajectories occurring in each cluster is also included.

At SIL and SBO, mean EC, OC, SO_4^{2-}, ^{210}Pb and K^+ concentrations associated with East-European air flows (cluster 6) were also significantly higher compared to the other clusters. These results indicate that these compounds could be transported from highly-polluted urban and industrial regions in East Europe towards central Europe, mainly during spring and fall, increasing the background concentrations registered there. Tscherwenka et al. (1998) showed that episodic high concentrations of SO_2 determined at SBO during spring, were associated with air masses that crossed high emission regions in Southeastern and Eastern European countries.

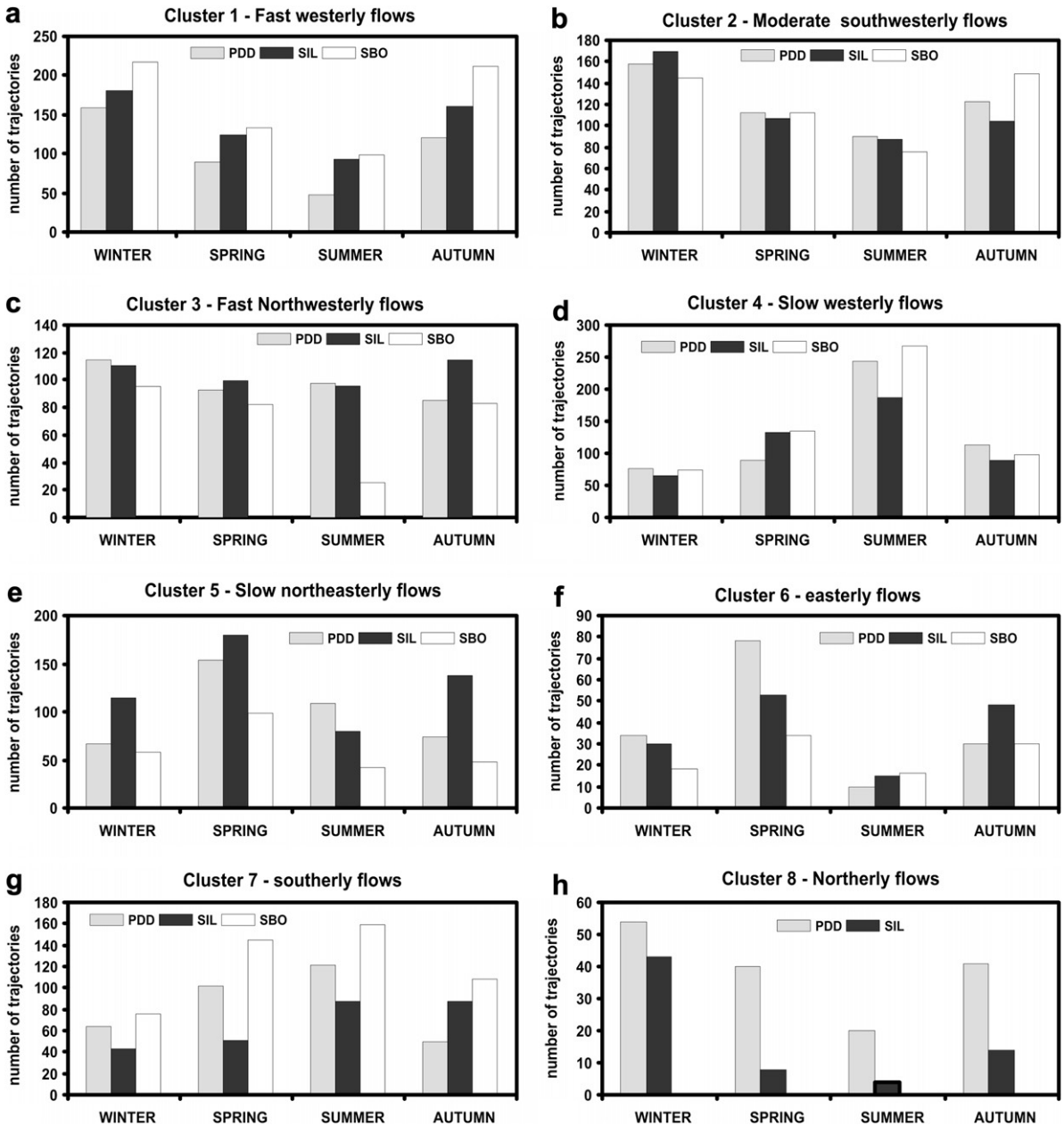

Fig. 3. Seasonal number of trajectories analysed for each cluster.

Mean EC, OC, SO_4^{2-}, ^{210}Pb and K^+ concentrations associated with cluster 7 at PDD, were also elevated. This was probably a consequence of pollutants emitted in the Mediterranean basin which were subsequently transported towards the continent. The western and central Mediterranean area and regions of southern France, Italy and the Balkan Peninsula, were previously identified as the main source areas of gaseous and particulate pollutants in the air of rural background monitoring stations in Spain (Rúa et al., 1998; Salvador et al., 2008). Additionally, commercial shipping is estimated to contribute 5–8% of global anthropogenic SO_2 emissions and 15–30% of global fossil fuel sourced NO*x* emissions (Eyring et al., 2005). The use of old engines in many ships and a very poor fuel quality containing high levels of sulphur and polyaromatic hydrocarbons, lead to the formation of large amounts of sulfate, soot particles and volatile hydrocarbon compounds from unburnt fuel and lubricant oil. For this reason, ship exhausts in highly trafficked areas such as the Mediterranean basin can generate substantially high levels of EC, OC and SO_4^{2-}. The levels of SO_4^{2-} during the summer are also probably increased by enhanced oxidation rates of marine DMS emissions in this area.

It should be noted that at SIL and PDD, mean Ca^{2+} and Na^+ concentrations levels associated with cluster 7 (North African air flows) and clusters 1 and 2 (maritime air masses) respectively, were significantly higher than in any of the other patterns. The Na^+ concentrations levels at SBO are far lower than at other sites and appear to be less sensitive to the different clusters. The fact that cluster 7 conditions favoured high PM10 Ca^{2+} concentrations at SIL and PDD, suggests that during the occurrence of long-range transport episodes of mineral dust from North Africa desert regions, the crustal load registered in the centre of Europe is increased. Previous studies have highlighted the incidence of transport episodes of highly dust loaded air masses from the Sahel and Sahara regions, on

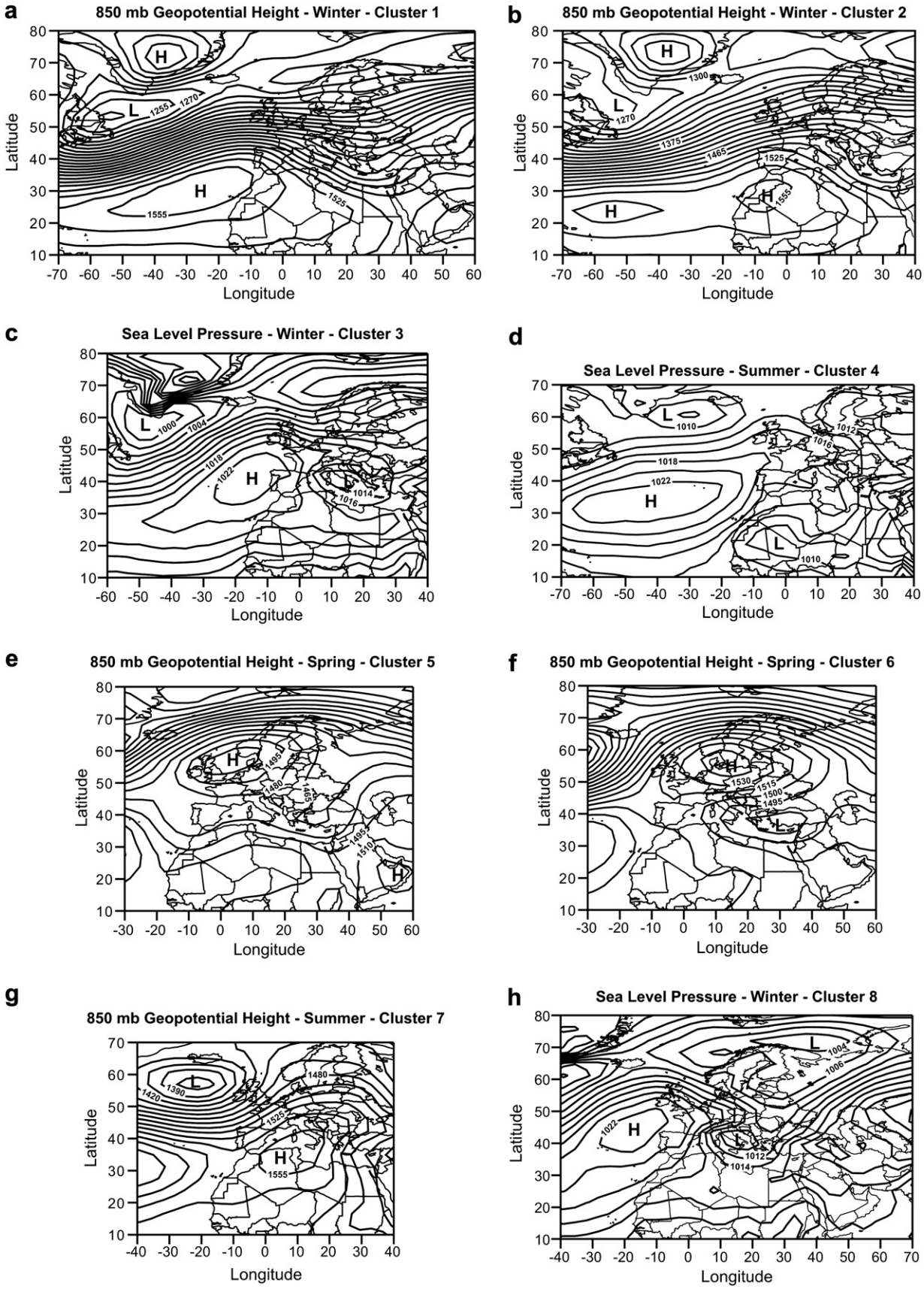

Fig. 4. Composite 850 mb geopotential height (m) or Sea Level Pressure (mb) for the trajectories of the clusters during their most frequently period of occurrence.

Table 1
Mean PM components concentrations for the different trajectory cluster identified at SIL, PDD and SBO. N, number of trajectories.

	N	EC	OC	SO_4^{2-}	Ca^{2+}	K^+	Na^+	^{210}Pb
		µgC m^{-3}	µgC m^{-3}	ng m^{-3}	ng m^{-3}	ng m^{-3}	ng m^{-3}	mBq m^{-3}
SIL-PM10	2944	0.29	2.40	2263	254	90	197	0.54
Cluster 1	558	0.23	1.66	1562	182	67	233	0.38
Cluster 2	467	0.25	2.14	2268	318	97	241	0.50
Cluster 3	456	0.29	2.35	2140	235	88	200	0.45
Cluster 4	476	0.31	2.93	2703	308	108	211	0.58
Cluster 5	511	0.35	2.97	2552	231	98	134	0.65
Cluster 6	137	0.37	2.71	2754	173	92	117	0.69
Cluster 7	270	0.29	2.74	2483	353	107	200	0.68
Cluster 8	69	0.20	1.38	1371	157	53	194	0.34
PDD-PM10	2884	0.22	1.51	1290	131	42	112	0.36
Cluster 1	416	0.16	0.75	696	72	22	107	0.20
Cluster 2	482	0.18	1.25	1168	129	36	138	0.30
Cluster 3	422	0.22	1.47	1126	117	36	106	0.31
Cluster 4	520	0.25	1.95	1716	188	53	137	0.45
Cluster 5	402	0.22	1.96	1519	154	51	87	0.40
Cluster 6	150	0.23	1.41	1175	86	43	63	0.38
Cluster 7	337	0.25	1.81	1675	173	55	117	0.48
Cluster 8	155	0.21	1.17	1107	103	34	88	0.28
SBO-PM2.5	2825	0.14	0.90	653	ND[a]	27	18	0.41
Cluster 1	662	0.09	0.63	537	–	18	14.6	0.32
Cluster 2	481	0.12	0.84	620	–	24	17.5	0.38
Cluster 3	278	0.10	0.68	517	–	18	11.2	0.34
Cluster 4	572	0.17	1.13	771	–	29	16.8	0.44
Cluster 5	246	0.19	1.01	717	–	31	17.7	0.41
Cluster 6	98	0.18	0.92	746	–	34	22.9	0.39
Cluster 7	488	0.14	0.98	685	–	29	16.5	0.39

[a] ND, Not Determined. Samples probably contaminated by construction activities using concrete.

the levels of mineral aerosol recorded in the south European countries (Bergametti et al., 1992; Kubilay et al., 2000; Salvador et al., 2008; Querol et al., 2008a and references therein). Otherwise, mineral dust is regularly deposited over the Alps in the course of Saharan air mass advections. Precipitation containing scavenged Saharan-dust is known as “red rain” or “yellow snow” and can be deposited in ice cores and ultimately preserved in glaciers. Saharan-dust bearing snow layers are characterized by extremely high amounts of $CaCO_3$ and gypsum (Wagenbach et al., 1996; Legrand et al., 2002; Sodemann et al., 2006).

In general, with the exception of Na^+, the statistical test results have shown that the lowest mean PM concentrations measured at SIL, PDD and SBO were associated with advections of Atlantic air masses (clusters 1, 2 and 8). This is a consequence of the relative weakness of oceanic sources of EC, OC, SO_4^{2-}, Ca^{2+}, K^+ and ^{210}Pb in comparison with continental sources. In addition, these atmospheric transport scenarios were frequently linked to frontal systems which gave rise to scavenging processes, such as high precipitation rates and strong winds, producing a drop in PM concentration levels.

3.2. RCF analysis results

RCF results are reported on geographical maps. For each cell of any map a weighted concentration of the component under study was computed using the procedure defined by Stohl (1996). To assess quantitatively the weighted concentrations, they were distributed in five equal intervals from the lowest to the highest values. Thus, cells with weighted concentrations in the higher and lower value ranges indicate that, on average, air parcels residing over these cells result in high and low concentrations of the component at the receptor site, respectively. RCF show concentration gradients across potential sources. Table 2 summarizes the main potential source areas obtained for each aerosol component and season. The geographic areas identified as the greatest potential source areas of the different PM compounds are: northern Africa, central Europe, southern Europe, northeastern Europe, eastern Europe, western Mediterranean, western and northwestern Russia, Ukraine and southwestern Russia, western Kazakhstan and the Urals and the Atlantic Ocean. RCF maps are discussed for the main aerosol components of PM10 (PDD and SIL) and PM2.5 (SBO) in Figs. 5 and 6.

RCF maps obtained for ^{210}Pb in PM10 (Fig. 5a-b) and PM2.5 (not shown) during the cold and the warm seasons were very similar. They clearly defined eastern Europe and northwestern Russia as the origin of the air masses that arrived at the centre of Europe, where their highest concentrations were obtained. The longer the transport of air masses over continental areas, the higher the ^{210}Pb concentration recorded at the monitoring sites. This pattern clearly correspond to an increase of ^{210}Pb concentration due to a continental pile up. During the warm season, the map also shows a contribution from central Europe (Fig. 5b). In this period, vertical air mass exchange was enhanced due to a more efficient mixing and upward transport from the boundary layer to the mountain sites. As stated before, the occurrence of slow and moderate moving flows was significantly higher during these months (Fig. 3). Thus, there was a higher contribution of the emissions from local and regional sources on the ^{210}Pb levels during the warmest months of the year. During the cold season the vertical mixing intensity was reduced. In the absence of breeze circulations that may transport upwards air parcels from the boundary layer, sites located at high altitudes are isolated from the surface sources of species most of the time. These results are not in contradiction with earlier findings. There is evidence that vertical mixing cannot be the only reason for an increase in gas and aerosol concentrations at SBO (Kasper and Puxbaum, 1998). During summer, when the mixing height was well above the SBO site, transports from the Po valley leaded to marked pollution events at SBO. However, their overall contribution to the observed concentrations of gaseous and aerosol species was much less pronounced (about 15% in summer and even less in winter, Seibert et al., 1998). Other phenomena such as medium- or long-range transport should be considered. A trajectory analysis revealed that long-range transport from strongly emitting regions in northeastern and southeastern Europe had

Table 2
Greatest potential source areas of PM components concentrations derived from the RCF analysis. Northern African (NAF), central Europe (CE: Germany, Austria, western Poland, Czech Republic, Holland, Belgium and northeastern France), southern Europe (SE: northern Italy, Swiss and southeastern France), northeastern Europe (NE: northern France and British Islands), eastern Europe (EE: the Baltic countries, Belarus and eastern Poland), western Mediterranean (WM), western and northwestern Russia (NWR), Ukraine and southwestern Russia (SWR), western Kazakhstan and the Urals (KUR), and the Atlantic Ocean (ATL).

	PM10		PM2.5	
	Warm period	Cold period	Warm period	Cold period
Ca^{2+}	NAF	NAF	ND[a]	SWR
^{210}Pb	CE–NWR	NWR	NWR–CE	SWR
Na^+	ATL–NAF–WM	ATL–NAF	SWR	SWR
SO_4^{2-}	CE–EE–WM	NWR–EE	CE–NE	SWR
EC	CE–EE–NWR	NWR	CE–SE	SWR
OC	CE	NWR	CE–SE	SWR–KUR
Oxalic	CE–WM	NWR–EE	ND	ND
Malonic	CE–WM	NWR–EE	ND	ND
K^+	CE	EE–NWR	CE–SE	KUR
Levoglucosan	ND	NWR	ND	KUR

[a] ND, Not Determined.

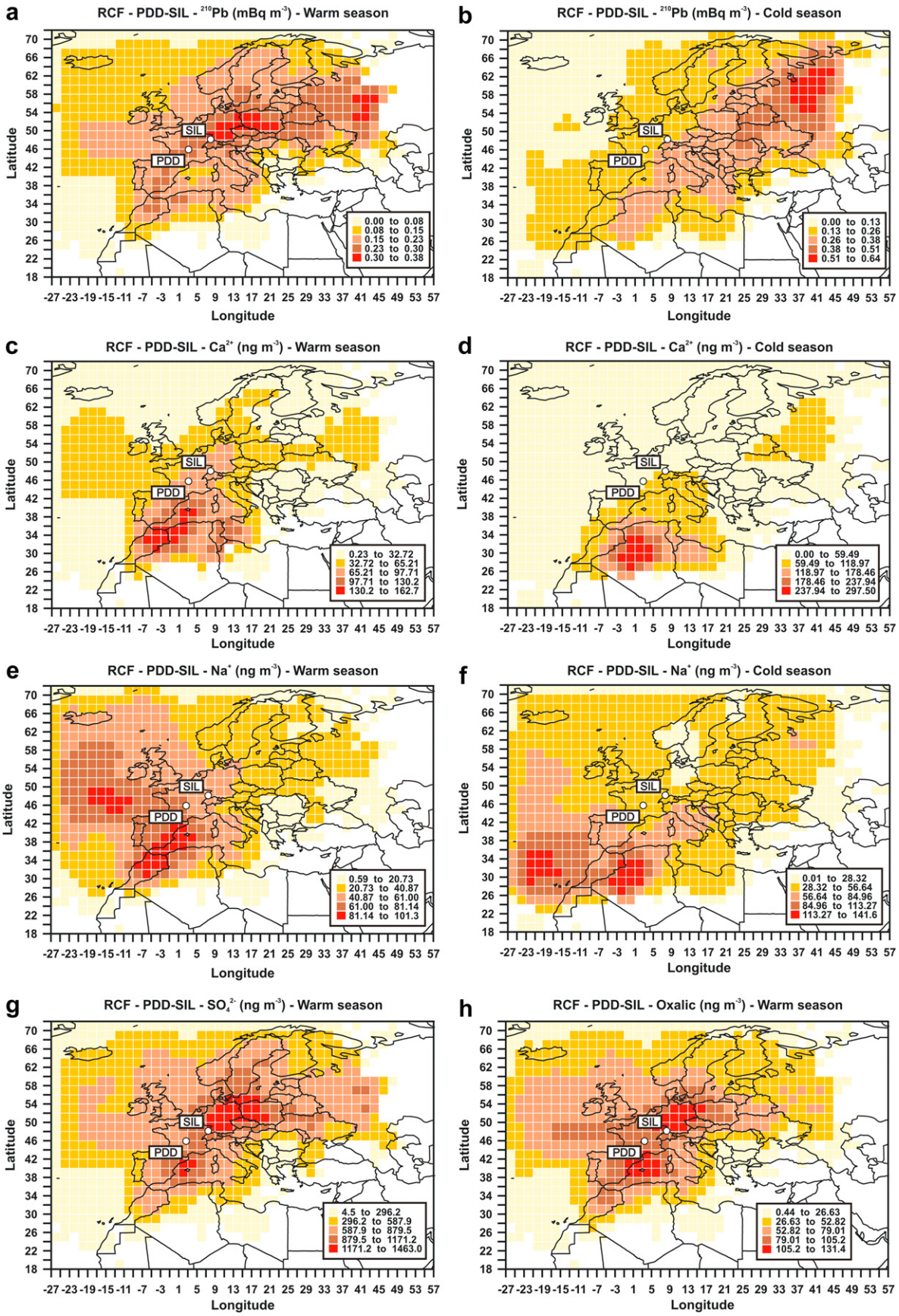

Fig. 5. RCF for selected components in PM10: ^{210}Pb, Ca^{2+} and Na^{+} during the warm (a, c, e) and the cold (b, d, f) seasons and SO_4^{2-} (g) and oxalic (h) during the warm season.

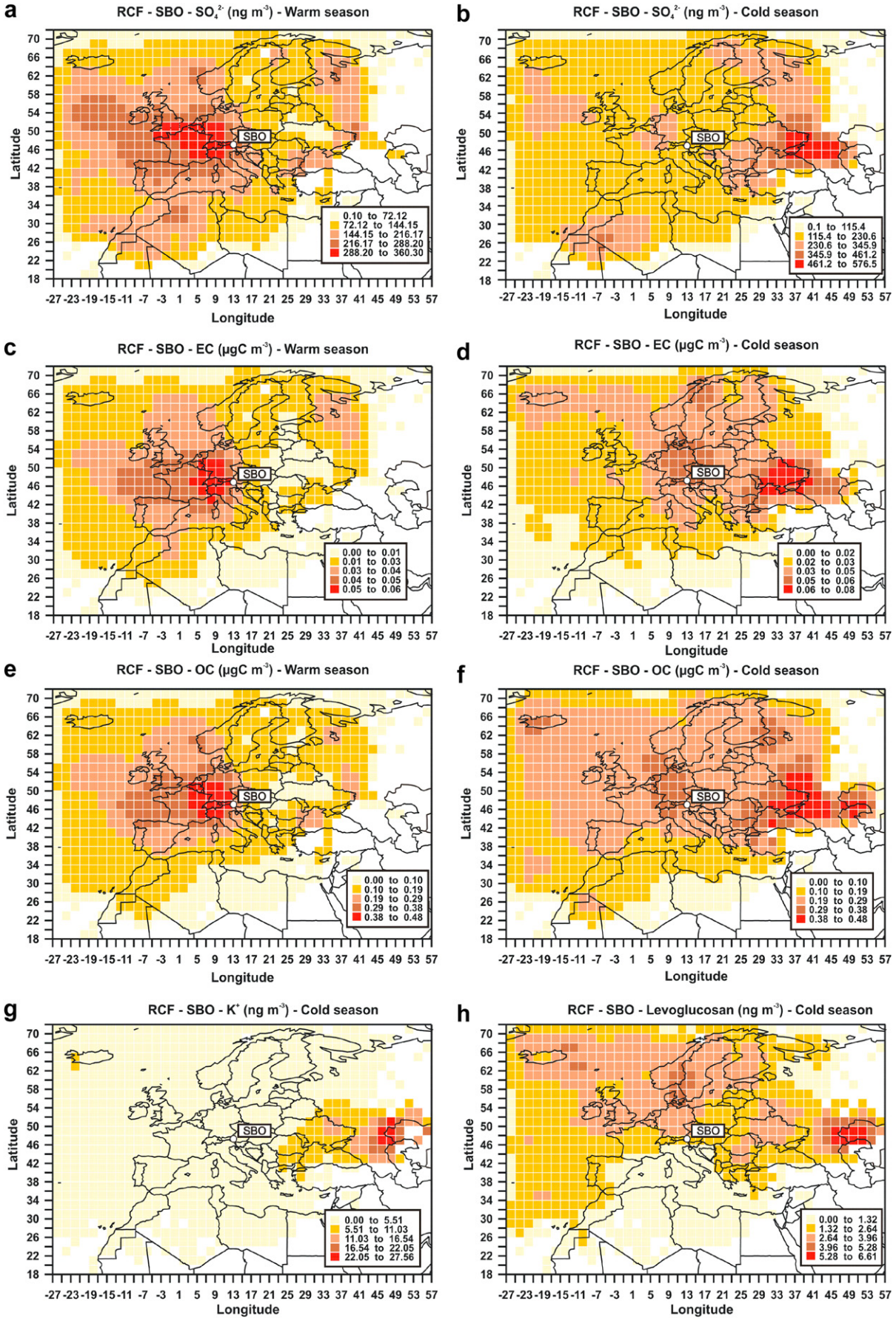

Fig. 6. RCF for selected components in PM2.5: SO_4^{2-}, EC and OC during the warm (a, c, e) and the cold (b, d, f) seasons and K^+ (g) and levoglucosan (h) during the cold season.

a clear impact on the amount of SO_2 determined at SBO, specially during early spring (Tscherwenka et al., 1998). Hammer et al. (2007) estimated that a large part of the spatiotemporal variability (~60%) of the secondary aerosol species (OC and anthropogenic sulfate) at these background sites may be attributed to transport processes. For this reason, the actual European baseline levels are registered at these sites during the winter months, the spatiotemporal variability of the pollutants concentrations being governed by air mass transport from distant regions (Querol et al., 2008b). This current finding highlights the impact of aged continental air masses on the background atmospheric load over central Europe, and shows the capabilities of the RCF technique for a rather consistent source apportionment of the aerosol components at the 3 European continental background locations studied.

Concerning the crustal source, the greatest potential contribution areas of Ca^{2+} for PDD–SIL were located in northern Africa throughout the year (Fig. 5c-d). The main potential source areas identified during the warm season were Morocco and the North of Libya while in the cold season was the centre of Libya.

RCF for Na^+ in PM10 defined different regions of Atlantic Ocean as well as northern Africa as the main potential source areas in both seasons (Fig. 5e-f). Dust plumes originating from Africa may be filled by sea salt during transport towards the site over the Mediterranean Sea (Sodemann et al., 2006). As discussed by Pio et al. (2007) another possibility is related to the fact that crustal aerosol also contains a small leachable fraction of Na^+. In marked contrast with the coarser fraction, other sources identified over central Europe and southwestern Russia, such as soil and manure-fertilized field emissions (Legrand et al., 2002) contributed to the highest concentrations of Na^+ registered at SBO (Table 2). However, mean levels of Na^+ recorded at SBO were quite low (Table 1), which makes it hard to detect the most relevant source areas.

In our study the main source regions of SO_4^{2-} detected by the trajectory statistics during the warm season were central Europe and west Mediterranean sea for PDD–SIL, and central, northeastern and southern Europe for SBO (Figs. 5g and 6a). The RCF distributions obtained for SO_4^{2-}, oxalic and other organic diacids in the warm period at PDD–SIL were very similar (Fig. 5g-h). The non-parametric Spearman rank-order correlation coefficient – r_s (Stohl, 1996; Charron et al., 1998) was computed between the concentrations in the grid cells of the maps of SO_4^{2-} and oxalic, to obtain a more quantitative comparison between the RCF maps. The value of this coefficient was 0.91. This suggests that during the warmest months, diacids were mainly produced secondarily.

The western Mediterranean basin was identified as an additional potential source area for SO_4^{2-} and diacids. As it was mentioned before, large amounts of particles and gases are emitted into the basin, mainly from shipping and other fossil fuel combustion sources. SO_4^{2-} and diacids in this area could also be produced by reactions involving marine biogenic emissions from DMS and phytoplankton (Legrand et al., 2007), respectively. There are also experimental evidences that, during air mass recirculation events produced under strong solar radiation, pollutants emitted into the basin are trapped into atmospheric reservoir layers. In these conditions high concentrations of oxidants, acidic compounds, aerosols and tropospheric ozone are produced (Millán et al., 1997; Gangoiti et al., 2006). The transport of photooxidants inland from the Spanish, French and Italian coasts has been documented by a number of works (Sandroni et al., 1994; Millán et al., 1997). In a recently published work, the Mediterranean area was identified as an important additional source for high ozone concentrations at high alpine sites during the summer months (Kaiser et al., 2007). Thus, under specific meteorological scenarios in the warm season such as the example represented in Fig. 7, this region could constitute an additional source area for the production of secondary aerosol. In this case the strong levels of subsidence generated a semipermanent high pressure area over the Balearic basin, which could transport the pollutants towards the NE direction.

In the cold season, the highest levels of SO_4^{2-} were observed over western and northwestern Russia and eastern Europe, at PDD–SIL, and over the Donestk coal basin in southwestern Russia (Fig. 6b), at the SBO site. The distribution of SO_2 emissions in Europe calculated by EMEP for the study period (http://www.ceip.at/emission-data-webdab/) identify these regions as high emission areas. Lignite brown coal is a major anthropogenic source of carbonaceous material and sulphur derived aerosol which has been widely used in the former eastern European block and the former USSR (Cooke et al., 1999).

Concerning EC, different results were obtained depending on the season. As for the case ^{210}Pb, discussed before, the seasonal cycle was mainly driven by the contrast of the regional-scale vertical mixing between the two seasons. During the warm season the highest level of EC were obtained over central/eastern Europe and northwestern Russia, for PDD–SIL, and central/southern Europe, for SBO (Fig. 6c). During the cold season the highest levels in the RCF were detected over northwestern/southwestern Russia, at PDD–SIL, and southwestern Russia, at SBO (Fig. 6d). The various source regions of EC, obtained for both seasons, agree with emission inventories and with well identified major industrial areas in Europe and Russia, such as the Volga and Ural industrial regions and the oil and gas complex in Western Kazakhstan (NILU, 1984; Olivier et al., 1996; Vinogradova, 2000; Vestreng, 2001; Lupu and Maenhaut, 2002). The central, northeastern and eastern parts of Europe have also been detected as the main NO_x and CO source regions contributing to the levels registered at high Alpine monitoring stations (Kaiser et al., 2007).

A source apportionment was carried out at the CARBOSOL sites by using a combination of organic chemical tracers and ^{14}C by

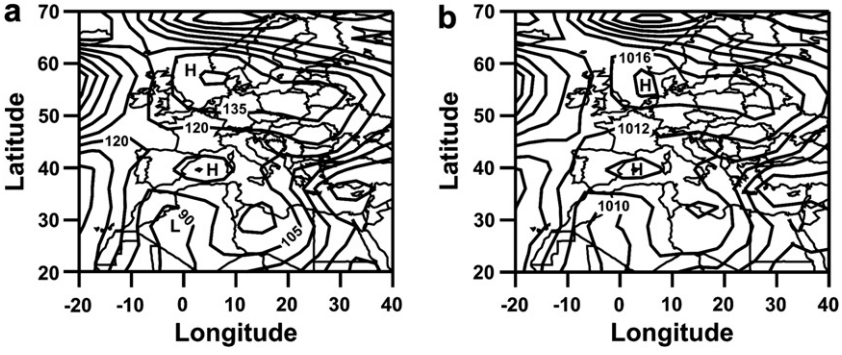

Fig. 7. Composite sea level pressure (mb) (a) and 1000 mb geopotential height (m) (b) for the period 29–31 May 2003 at 12:00 h UTC.

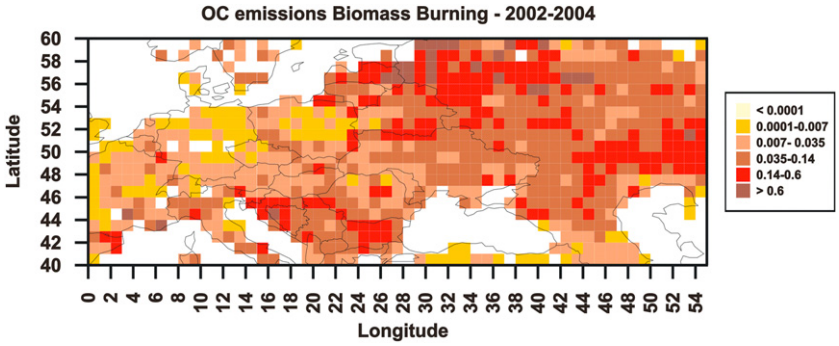

Fig. 8. Accumulated emissions of OC from wildfires (source: GFEDv2 database) in gOC m^{-2} over the period 2002–2004.

Gelencsér et al. (2007). They estimated that at PDD, SIL and SBO, the emissions of EC were dominated by fossil fuel combustion (80–94% and 95–97% of the total mass of EC in the cold and warm seasons, respectively). The value of r_s was higher than 0.89 for the comparison between EC and SO_4^{2-} in PM10 and PM2.5 during the cold season; this points to fossil fuel combustion as a major anthropogenic source of EC and sulfate aerosol in the eastern Europe, the emissions of which are likely transported towards central Europe during the cold season.

In the case of OC the region covering central/southern Europe was associated with the highest OC concentrations obtained at PDD–SIL and SBO during the warm season (Fig. 6e). The highest contributions to OC corresponded to non-fossil SOA attributed to biogenic VOCs, especially during the warm season (between 75 and 80% of the total mass of OC), in the source apportionment study of Gelencsér et al. (2007). Biogenic emissions from vegetation are also thought to be major precursors of organic diacids at these mountain sites (Legrand et al., 2007). Particularly high summer levels of dicarboxylic acids were recorded at SIL located in the Black Forest. During the warmest months, diacids were mainly secondarily produced and provided a good signature of the SOA formation.

During winter significant contributions of primary organic aerosol from biomass burning are expected at the three sites (between 12 and 17% of the total OC mass, Gelencsér et al., 2007). In this work we have accounted for the global distribution of total OC emissions from biomass burning using the Global Fire Emission Database version 2 (GFEDv2) (Van der Werf et al., 2006). This database provides monthly emissions from biomass burning on a global scale ($1^\circ \times 1^\circ$). The OC emissions aggregated for the sampling period in the RCF grid domain are displayed in Fig. 8, which shows large OC emissions from biomass burning in Baltic countries, Byelorussia, western Russia and Kazakhstan. The areas corresponding to Baltic countries, Byelorussia, and western Russia agree fairly well with maxima in the RCF obtained for OC, K^+ and levoglucosan, in winter at PDD-SIL. OC emissions from Kazakhstan accounted for the highest concentrations in the RCF computed for OC, K^+ and levoglucosan, at SBO (Fig. 6f–h). The value of r_s ranged from 0.94 to 0.97 for the comparison between OC and K^+, and from 0.87 to 0.88 for the comparison between OC and levoglucosan, in this period, at PDD–SIL and SBO. It suggests that long-range transport processes of PM, produced during biomass burning processes in these regions, have impact on surface PM levels recorded in the centre of Europe.

4. Conclusions

In this work different trajectory statistical methods have been applied to describe the main air mass flow patterns over central Europe and interpret the levels of the aerosol chemical components recorded at three remote background sites in this area. Their main potential source areas have also been geographically identified. A clear seasonal pattern has been observed at the three sites. During summer the highest EC, OC, SO_4^{2-}, K^+ and ^{210}Pb concentrations were associated with slow and moderate moving flows. The highest potential source regions were obtained over central European regions. In this season the vertical air mass exchange was enhanced by a more efficient mixing and upward transport from the boundary layer to the mountain sites, whereas the prevalent synoptic meteorological situations favoured regional transport from distant sources and the formation of secondary organic and inorganic aerosol by the photo-oxidation of biogenic emissions and, to a lesser extent, fossil fuel emissions. Meteorological scenarios represented by trajectories coming from the Mediterranean basin and North-Africa have also occurred frequently during the summer months. There is a growing body of evidence that the western Mediterranean basin is also a potential source of SO_4^{2-} and diacids. However, due to the high complexity of the photooxidant dynamics and the atmospheric circulations involved, this finding needs to be further explored. Besides, emissions from desert regions in North Africa seemed to significantly influence the central European background mineral aerosol concentrations throughout the year.

In winter, the lowest mean PM concentrations, except for Na^+, were observed. Advections of Atlantic air masses were the most frequent transport scenario. Under these conditions there is transport of sea salt particles inland, but low emissions over the Ocean and the efficient atmospheric scavenging of aerosol contributes to the observed low levels. In addition, in winter the background sites located at high altitudes were strongly decoupled from local and regional nearby surface continental aerosol sources.

In spring and autumn, the highest mean EC, OC, SO_4^{2-}, K^+ and ^{210}Pb aerosol concentrations in central Europe were likely caused by long-range transport PM contributions. Results obtained with tracers of biomass burning (K^+ and levoglucosan) and fossil fuel combustion (SO_4^{2-}) suggested the existence of long-range transport processes of OC and EC emissions produced by fossil fuel and biomass burning processes in the Baltic countries, Byelorussia, western regions of Russia and Kazakhstan. The statistical analysis applied on the concentration values of the continental transport tracer ^{210}Pb highlighted the influence of the aged continental air masses on the background atmospheric load in the centre of Europe, revealing an increase of PM concentrations due to a continental pileup.

Thus, the findings disclosed in this work suggest that air mass transport from natural and anthropogenic sources located far away from sites influence the background levels of PM registered in central Europe. The scientific evidence indicating that long-range transport of pollution is a major contributor to ambient levels of PM and population exposure (WHO, 2006) encourages international

actions and collaborations for further reduction of PM levels in Europe. The predominant meteorological scenarios that give rise to all of these transport episodes have been described. Further investigation is needed to understand the role of PM transport episodes on human health effects. However, the information provided in this paper can be used as a complementary tool for their prediction, analysis and interpretation.

Acknowledgements

This work was financed by the Spanish Ministry of Science and Innovation through the Acción Integrada HP2006-0034. The data from Schauinsland, Puy de Dôme and Sonnblick used in this study were obtained as part of project CARBOSOL (EVK2-2001-113), which was supported by the European Commission. ECMWF and NILU are acknowledged for providing the data sets and the FLEXTRA trajectories computed from Schauinsland and Puy de Dôme (www.nilu.no/trajectories/). The developers of the FLEXTRA model (Andreas Stohl, Gerhard Wotawa and Petra Seibert) are also acknowledged. The authors would like to thank the NOAA/OAR/ESRL PSD, Boulder, Colorado, USA for providing the meteorological dataset files (www.cdc.noaa.gov/). The authors are also very grateful to August Kaiser from the Central Institut for Meteorology and Geophysics of Vienna, Austria who provided the trajectories computed from Sonnblick, Dra. Marta García for her support in the composition of Fig. 1 and two anonymous referees for their valuable comments.

References

Bergametti, G., Remoudaki, E., Losno, R., Steiner, E., Chatenet, B., Buat-Ménard, P., 1992. Source, transport and deposition of atmospheric phosphorus over the northwestern Mediterranean. Journal of Atmospheric Chemistry 14, 501–513.

Brankov, E., Rao, S.T., Porter, P.S., 1998. A trajectory-clustering-correlation methodology for examining the long-range transport of air pollutants. Atmospheric Environment 32, 1525–1534.

Charron, A., Plaisance, H., Sauvage, S., Coddeville, P., Galloo, J.C., Guillermo, R., 1998. Intercomparison between three receptor-oriented models applied to acidic species in precipitation. The Science of the Total Environment 223, 53–63.

Cooke, W.F., Liousse, C., Cachier, H., 1999. Construction of a $1^\circ \times 1^\circ$ fossil fuel emission data set for carbonaceous aerosol and implementation and radiative impact in the ECHAM4 model. Journal of Geophysical Research 104 (D18), 22137–22162.

Dorling, S.R., Davies, T.D., Pierce, C.E., 1992. Cluster analysis: a technique for estimating the synoptic meteorological controls on air and precipitation chemistry – method and applications. Atmospheric Environment 26A, 2575–2581.

Eyring, V., Kohler, H.W., van Aardenne, J., Lauer, A., 2005. Emissions from international shipping: 1. The last 50 years. Journal of Geophysical Research 110, D17305. doi:10.1029/2004JD005619.

Fagerli, H., Legrand, M., Preunkert, S., Vestreng, V., Simpson, D., Cerqueira, M., 2007. Modeling historical long-term trends of sulfate, ammonium, and elemental carbon over Europe: a comparison with ice core records in the Alps. Journal of Geophysical Research 112, D23S13. doi:10.1029/2006JD008044.

Gangoiti, G., Alonso, L., Navazo, M., García, J.A., Millán, M.M., 2006. North African soil dust and European pollution transport to America during the warm season: hidden links shown by a passive tracer simulation. Journal of Geophysical Research 111, D10109. doi:10.1029/2005JD005941.

Gelencsér, A., May, B., Simpson, D., Sanchez-Ochoa, A., Kasper-Giebl, A., Puxbaum, H., Caseiro, A., Pio, C.A., Legrand, M., 2007. Source apportionment of PM2.5 organic aerosol over Europe: primary/secondary, natural/anthropogenic, and fossil/biogenic origin. Journal of Geophysical Research 112, D23S04. doi:10.1029/2006JD008094.

Hammer, S., Wagenbach, D., Preunkert, S., Pio, C.A., Schlosser, C., Meinhardt, F., 2007. Lead-210 observations within CARBOSOL: a diagnostic tool for assessing the spatiotemporal variability of related chemical aerosol species? Journal of Geophysical Research 112, D23S03. doi:10.1029/2006JD008065.

Han, Y., Holsen, T.M., Hopke, P.K., Cheong, J., Kim, H., Yi, S., 2004. Identification of source locations for atmospheric dry deposition of heavy metals during yellow-sand events in Seoul, Korea in 1998 using hybrid receptor models. Atmospheric Environment 38, 5353–5361.

Jorba, O., Pérez, C., Rocadenbosch, F., Baldasano, J.M., 2004. Cluster analysis of 4-day back trajectories arriving in the Barcelona area, Spain, from 1997 to 2002. Journal of Applied Meteorology 43, 887–901.

Kaiser, A., Scheifinger, H., Spangl, W., Weiss, A., Gilge, S., Fricke, W., Ries, L., Cemas, D., Jesenovec, B., 2007. Transport of nitrogen oxides, carbon monoxide and ozone to the alpine global atmosphere Watch stations Jungfraujoch (Switzerland), Zugspitze and Hohenpeissenberg (Germany), Sonnblick (Austria) and Mt. Krvavec (Slovenia). Atmospheric Environment 41, 9273–9287.

Kalnay, E., Kanamitsu, M., Kistler, R., Collins, W., Deaven, D., Gandin, L., Iredell, M., Saha, S., White, G., Woollen, J., Zhu, Y., Chelliah, M., Ebisuzaki, W., Higgins, W., Janowiak, J., Mo, K.C., Ropelewski, C., Wang, J., Leetmaa, A., Reynolds, R., Jenne, R., Joseph, D., 1996. The NCEP/NCAR 40-year reanalysis project. Bulletin of the American Meteorological Society 77, 437–470.

Kasper, A., Puxbaum, H., 1998. Seasonal variation of SO_2, HNO_3, NH_3 and selected aerosol components at Sonnblick (3106 m a.s.l. Atmospheric Environment 32, 3925–3939.

Kubilay, N., Nickovic, S., Moulin, C., Dulac, F., 2000. An illustration of the transport and deposition of mineral dust onto the eastern Mediterranean. Atmospheric Environment 34, 1293–1303.

Legrand, M., Puxbaum, H., 2007. Summary of the CARBOSOL project: present and retrospective state of organic versus inorganic aerosol over Europe. Journal of Geophysical Research 112. doi:10.1029/2006JD008271.

Legrand, M., Preunkert, S., Wagenbach, D., Fischer, H., 2002. Seasonally resolved Alpine and Greenland ice core records of anthropogenic HCl Emissions over the 20th century. Journal of Geophysical Research 107, D12. doi:10.1029/2001JD001165.

Legrand, M., Preunkert, S., Oliveira, T., Pio, C.A., Hammer, S., Gelencsér, A., Kasper-Giebl, A., Laj, P., 2007. Origin of C2–C5 dicarboxylic acids in the European atmosphere inferred from year-round aerosol study conducted at a west–east transect. Journal of Geophysical Research 112, D23S07. doi:10.1029/2006JD008019.

Lupu, A., Maenhaut, W., 2002. Application and comparison of two statistical trajectory techniques for identification of source regions of atmospheric aerosol species. Atmospheric Environment 36, 5607–5618.

Millán, M.M., Salvador, R., Mantilla, E., Kallos, G., 1997. Photo-oxidant dynamics in the Mediterranean basin in summer: results from European research projects. Journal of Geophysical Research 102, 8811–8823.

NILU, 1984. Emission Sources in the Soviet Union. Technical Report 4/84. The Norwegian Institute for Air Research, Lillestrom.

Olivier, J.G.J., Bouwman, A.F., van der Mass, C.W.M., Berdowski, J.J.M., Veldt, C., Bloss, J.P.J., Vesschedijk, A.J.H., Zandveldt, P., Haverlag, J., 1996. Description of EDGAR Version 2.0: A Set of Global Emission Inventories of Greenhouse Gases and Ozone-Depleting Substances for all Anthropogenic and most Natural Sources on a per Country Basis and on $1^\circ \times 1^\circ$ grid. RIVM/TNO Report 771060 022. Rijkinstituut voor Volksgezondheid en Milieu, Bilthoven, Netherlands.

Owen R.C. (2003). A Climatological study of transport to the PICO-NARE site using atmospheric backward trajectories. Civil and environmental Engineering, Michigan Technological University, Master of Science, Houghton, MI, 361 pp.

Pio, C.A., Legrand, M., Oliveira, T., Afonso, J., Santos, C., Caseiro, A., Fialho, P., Barata, F., Puxbaum, H., Sanchez-Ochoa, A., Kasper-Giebl, A., Gelencsér, A., Preunkert, S., Schock, M., 2007. Climatology of aerosol composition (organic versus inorganic) at nonurban sites on a west-east transect across Europe. Journal of Geophysical Research 112, D23S02. doi:10.1029/2006JD008038.

Puxbaum, H., Caseiro, A., Sanchez-Ochoa, A., Kasper-Giebl, A., Claeys, M., Gelencsér, A., Legrand, M., Preunkert, S., Pio, C.A., 2007. Levoglucosan levels at background sites in Europe for assessing the impact of biomass combustion on the European aerosol background. Journal of Geophysical Research 112, D23S05. doi:10.1029/2006JD008114.

Querol, X., Alastuey, A., Moreno, T., Viana, M.M., Castillo, S., Pey, J., Rodriguez, S., Artiñano, B., Salvador, P., Garcia do Santos, S., Herce Garraleta, M.D., Fernandez Patier, R., Moreno, S., Minguillón, M.C., Monfort, E., Palomo, R., Pinilla, E.R., Cuevas, E., 2008a. Spatial and temporal variations in airborne particulate matter (PM10 and PM2.5) across Spain 1999–2005. Atmospheric Environment 42, 3964–3979.

Querol, X., Alastuey, A., Moreno, T., Viana, M.M., 2008b. New directions: legislative considerations for controlling exposure to atmospheric aerosols in rural areas. Atmospheric Environment 42, 8979–8984.

Rúa, A., Hernández, E., de las Parras, J., Martín, I., Gimeno, L., 1998. Sources of SO_2, SO_4^{2-}, NO_x and NO_3^- in the air of four Spanish remote stations. Journal of the Air and Waste Management Association 48, 838–845.

Salvador, P., Artíñano, B., Querol, X., Alastuey, A., Costoya, M., 2007. Characterisation of local and external contributions of atmospheric particulate matter at a background coastal site. Atmospheric Environment 41, 1–17.

Salvador, P., Artíñano, B., Querol, X., Alastuey, A., 2008. A combined analysis of backward trajectories and aerosol chemistry to characterise long-range transport episodes of particulate matter: the Madrid air basin, a case study. Science of the Total Environment 390, 495–506.

Sandroni, S., Bacci, P., Boffa, G., Pellegrini, U., Ventura, A., 1994. Tropospheric ozone in the pre-alpine and alpine regions. Science of the Total Environment 516 (2), 169–182.

Seibert, P., Kromp-Kolb, H., Hasper, A., Kalina, M., Puxbaum, H., Jost, D.T., Schwikowski, M., Baltensperger, U., 1998. Transport of polluted boundary layer air from the Po valley to high-alpine sites. Atmospheric Environment 32, 3953–3965.

Simpson, D., Yttri, K.E., Klimont, Z., Kupiainen, K., Caseiro, A., Gelencsér, A., Pio, C.A., Puxbaum, H., Legrand, M., 2007. Modeling carbonaceous aerosol over Europe: analysis of the CARBOSOL and EMEP EC/OC campaigns. Journal of Geophysical Research 112, D23S14. doi:10.1029/2006JD008158.

Sodemann, H., Palmer, A.S., Schwierz, C., Schwikowski, M., Wernli, H., 2006. The transport history of two Saharan dust events archived in an Alpine ice core. Atmospheric Chemistry and Physics 6, 667–688.

Stohl, A., Wotawa, G., Seibert, P., Kromp-Kolb, H., 1995. Interpolation errors in wind fields as a function of spatial and temporal resolution and their impact on different types of kinematic trajectories. Journal of Applied Meteorology 34, 2149–2165.

Stohl, A., 1996. Trajectory statistics-a new method to establish source-receptor relationships of air pollutants and its application to the transport of particulate sulfate in Europe. Atmospheric Environment 30, 579–587.

Stohl, A., 1998. Computation, accuracy and applications of trajectories – a review and bibliography. Atmospheric Environment 32, 947–966.

Tscherwenka, W., Seibert, P., Kasper, A., Puxbaum, H., 1998. On-line measurements of sulfur dioxide at the 3 km level over central Europe (Sonnblick observatory, Austria) and statistical trajectory source analysis. Atmospheric Environment 32, 3941–3952.

Tsyro, S., Simpson, D., Tarrasón, L., Klimont, Z., Kupiainen, K., Pio, C.A., Yttri, K.E., 2007. Modeling of elemental carbon over Europe. Journal of Geophysical Research 112, D23S19. doi:10.1029/2006JD008164.

Van der Werf, G.R., Randerson, J.T., Giglio, L., Collatz, G.J., Kasibhatla, P.S., 2006. Interannual variability in global biomass burning emissions from 1997 to 2004. Atmospheric Chemistry and Physics 6, 3423–3441.

Venzac, H., Sellegri, K., Villani, P., Picard, D., Laj, P., 2009. Seasonal variation of aerosol size distributions in the free troposphere and residual layer at the puy de Dôme station, France. Atmospheric Chemistry and Physics 9, 1465–1478.

Vestreng, V., 2001. Emission Data Reported to UNECE/EMEP: Evaluation of the Spatial Distribution of Emissions. EMEP/MSC-W Note 1/01. The Norwegian Meteorological Institute, Oslo (July).

Viana, M., Kuhlbusch, T.A.J., Querol, X., Alastuey, A., Harrison, R.M., Hopke, P.K., Winiwarter, W., Vallius, M., Szidat, S., Prévôt, A.S.H., Hueglin, C., Bloemen, H., Wahlin, P., Vecchi, R., Miaranda, A.I., Kasper-Giebl, A., Maenhaut, W., Hitzenberger, R., 2008. Source apportionment of particulate matter in Europe: a review of methods and results. Journal of Aerosol Science 39, 827–849.

Vinogradova, A.A., 2000. Anthropogenic pollutants in the Russian Arctic atmosphere: sources and sinks in spring and summer. Atmospheric Environment 34, 5151–5160.

Wagenbach, D., Preunkert, S., Schafer, J., Jung, W., Tomadin, L., 1996. Northward transport of Saharan dust recorded in a deep Alpine ice core. In: Guerzoni, S., Chester, R. (Eds.), The Impact of African Dust across the Mediterranean. Kluwer Academic Publishers, Dordrecht, pp. 291–300.

WHO, Joint WHO/Convention Task Force on the Health Aspects of Air Pollution, 2006. Health Risks of Particulate Matter from Long-range Transboundary Air Pollution. European Centre for Environment and Health, Bonn Office. 99 pp.

Wotawa, G., Kröger, H., 1999. Testing the ability of trajectory statistics to reproduce emission inventories of air pollutants in cases of negligible measurement and transport errors. Atmospheric Environment 33, 3037–3043.